A TABULATED CHEMISTRY MODEL FOR NON-PREMIXED COMBUSTION AT HIGH PRESSURE SUPERCRITICAL CONDITIONS

Guilhem Lacaze[a,b] , **Joseph Oefelein**[b]

[a]gnlacaz@sandia.gov
[b]Sandia National Laboratories, Livermore, CA, 94550, USA

Abstract

This study presents the comprehensive development of a combustion model for turbulent non-premixed flames at high-pressure supercritical conditions. Emphasis is placed on flame stability in liquid rocket engines, with liquid-oxygen and gaseous hydrogen as the propellants. In such devices, combustion is affected by strain, pressure and heat-loss processes. Flame sensitivity to these processes is studied to define the most appropriate combustion model. Steady opposed-jet flames were used to study the flame structure under rocket-like conditions. The primary focus was liquid-oxygen–hydrogen flame topology and sensitivity. It is shown that the flame is very robust to strain, that the flamelet assumption is valid for the conditions of interest, and that real-fluid phenomena can have a significant impact on flame structure near the critical point. In this thermodynamic state, small pressure or temperature variations can induce significant variations of the temperature profile across the flame. A key objective of this work is to investigate how these effects can be taken into account in the modeling context. Resultant observations were used to develop a model framework that combines detailed thermodynamics with a tabulated chemistry approach. Flame structure is represented as a source term to preserve the solver's ability to capture compressibility and heat-loss effects. The model correctly reproduces the effects of strain, pressure and temperature on flame sensitivity . It is also demonstrated that the approach preserves the density gradient in the high-shear region between the liquid-oxygen jet and product rich flame region. The latter is a key requirement to properly simulate dense-fluid jet destabilization and mixing in practical devices.

1. Introduction

Practical devices such as gas turbines, diesel engines, and rockets operate at elevated pressures that approach and/or exceed the thermodynamic critical point of the propellants. Under these conditions, injected liquid jets undergo a transcritical change of state as fluid temperatures rise above the critical temperature of the local mixture. For this situation, diminished inter-molecular forces promote diffusion dominated mixing processes prior to atomization and injected jets vaporize in the presence of exceedingly large thermophysical gradients. Well-mixed diffusion flames evolve as a consequence and intense property gradients approach the behavior of a contact discontinuity. Significant real-gas effects and transport anomalies coexist locally in colder regions of the flow, with ideal gas and transport processes occurring within the flame zone [20]. The focus for the present work is development of a combustion model for use with the Large Eddy Simulation (LES) technique [2, 11, 13, 14]. The goal is to facilitate studies of flame stability in rocket engines fueled with liquid propellants (oxygen and hydrogen) at high pressure. In this type of application, propellants are injected separately and flames are located

within the mixing regions. Average pressures in the chamber are 70 *bar*, which is above the critical pressures of both reactants ($P_{O_2}^c = 50.4$ *bar* and $P_{H_2}^c = 12.9$ *bar* [9]). In addition to a predictive combustion model, sophisticated models to deal with thermodynamics and transport are required and must be an itegral part of the model formulation. The ultimate objective of this work is to develop a combustion model able to capture all processes involved.

Previous experimental studies at conditions relevant to liquid rocket have shown that the combustion of hydrogen and oxygen occurs in a nonpremixed regime [3, 10, 21, 22]. Candel and colleagues [3] have shown that the flame remains attached to the injector over a large range of pressure, inlet velocities, and hydrogen temperatures, with no local extinction observed in the flame sheet. Detailed simulations have provided additional understandings. Juniper *et al.* [7] studied in detail the stabilization mechanisms of $LOX - GH_2$ (liquid oxygen - gaseous hydrogen) flames at various conditions. Three parameters were examined in particular; the Damköhler number, the Spalding number, and aspects related to the injector tip geometry. The thickness of the LOX post was found to be the most influential. When this thickness is large compared to the reaction thickness, the flame is stabilized. Otherwise, the flame is exposed to the freestream and is very sensitive to the Damköhler number or the vortex shedding from the step. The inner structure of $LOX - H_2$ flames has been studied by Ribert *et al.* [21] and Juniper *et al.* [8]. Laminar counter-flow flames were studied at various pressure and strain rates conditions. It was shown that the flame is very robust to strain over a large range of pressures at both sub- and super-critical conditions.

Results to date suggest that H_2/O_2 flames at supercritical pressure can be model using a flamelet approach with tabulated chemistry. To verify this assumption, the exact flame structure must be studied along with its sensitivity to strain, pressure, and temperature variations encountered in the chamber. This task is not trivial since thermodynamics and mixing processes are much more complex at high pressures compared to low pressures where gases can be assumed ideal. Given this facts, the objectives of this paper are:

- To study the structure of the hydrogen-oxygen flames at transcritical conditions.

- To establish a systematic approach for development of a valid combustion model at these conditions.

- To test the model's response to strain, pressure and temperature variations.

The theoretical and numerical framework is presented in the next section followed by analysis of the flame structure in the third section. In Section 4, findings from the previous sections are used to formulate the combustion model. In the final section, a systematic assessment of the model is performed through comparisons with a series of detail computational results. Note that issues related to the turbulence closure itself is not discussed here since the study is focused on aspects of the model formulation related to tabulation of laminar flame properties. Comments on this point will be addressed at the end of the paper.

2. Theoretical basis and numerical approach

The theoretical and numerical framework of the present study has been developed by Oefelein [15, 16]. This framework has been optimized to meet the algorithm requirements imposed by the LES formalism and was defined to provide an unified treatment of high Reynolds-number, high-pressure, real-gas/liquid, reacting flows over a wide Mach operating range. To maintain page limitations, the governing system of equations are not presented here and the

reader is referred to [16] for more details. These equations are coupled using a cubic equation of state [20] and appropriate treatments of thermodynamic and transport properties to capture correctly supercritical effects occurring at high pressures.

2.1. Equation of state and thermodynamic properties

The equation of state employed in the present study is the Peng-Robinson (*PR*) cubic equation [20]:

$$P = \frac{RT}{V-b} - \frac{a}{V^2 + 2bV - b^2},$$

(1)

where R is the ideal-gas constant and V the molar volume. The coefficients a and b are coefficients that account for attraction and repulsion effects among molecules. They are calculated using a set of nonlinear mixing-rules that can be found in Reid *et al.* [20, Chapter 4]. This equation has been chosen because it is more more suitable for conditions when the temperature is greater than the critical temperature, which is the case in the flame. A summary of the cubic equations of state and recommended constants is also given by Reid *et al.* [20, Chapter 3].

A property evaluation scheme developed by Oefelein [17] is used to determine the thermodynamic properties. Having established an analytical representation for real mixture *p-v-T* behavior, the thermodynamic properties are obtained in two steps. First, respective component properties are combined at a fixed temperature using the corresponding states methodology to obtain the mixture state at a given reference pressure. A pressure correction is then applied using departure functions of the form given by Reid et al. [20, Chapter 5]. These functions are exact relations derived using the Maxwell relations and make full use of the real mixture *p-v-T* path dependencies dictated by the equation of state.

2.2. Transport Properties

At supercritical pressures, classical methods to determine transport properties do not apply. Mixing between dense and light fluids depend on molecular interactions, which differ from classical two-phase flow processes. Hence, an accurate formalism for the evaluation of transport coefficients is required. Molecular transport properties are evaluated in a manner analogous to the thermodynamic properties. Viscosity and thermal conductivity are obtained using the extended corresponding states methodologies developed by Ely and Hanley [4]. Mass and thermal diffusion coefficients are obtained using methodologies from the work of Hirschfelder et al. [6] and Takahashi [23]. This approach can handle general systems where multicomponent and/or preferential diffusion processes are present.

2.3. Chemical Kinetics and Source Term Closure

For the present study, a finite-rate hydrogen-oxygen kinetics is employed using the nine species (H_2, O_2, OH, H_2O, H, O, HO_2, H_2O_2, N_2), 19-step mechanism developed by of Ó-Conaire et al. [12]. One of the main objectives of this work is to study the flame structure of oxygen-hydrogen at elevated pressure. Hence the flame is completely resolved on the grid and no turbulent closure is required.

2.4. Numerical approach

The governing system is discretized on a staggered grid in generalized curvilinear coordinates. This formulation provides non-dissipative spectrally clean damping characteristics and discrete conservation of mass, momentum and total-energy. Integration is performed using a unique dual-time multistage scheme with a generalized all-Mach-number preconditioning methodology that optimally treats convective, diffusive, geometric, and source term anomalies

in a unified manner. The implicit formulation is A-stable, which allows one to set the physical timestep based solely on accuracy considerations. The scheme accommodates any arbitrary equation of state. The algorithm has been optimized to provide excellent parallel scalability attributes using a distributed multiblock domain decomposition with generalized connectivity. Inlet and outlet boundary conditions are treated using the method of characteristics [19].

3. Flame structure study

A classical method to study the flame structure of nonpremixed combustion is to stabilize the flames between two opposed jets, one fuel and the other oxidizer. In the present context, the characteristic timescale of chemistry is much smaller than turbulence and pressure oscillations and the steady flamelet assumption applies. Thus, two-dimensional steady laminar opposed-jet calculations are a valid method to study the flame structure.

Figure 1a) shows a diagram of the configuration, where a fuel rich laminar jet interacts with an opposed oxidizer rich laminar jet. A nonpremixed flame is stabilized near the stagnation point. The strain applied to the flame mimics the effect of a turbulent eddy forcing the flow toward the flame. The shape of the numerical domain is defined using potential flow theory. Based on this theory, the equations of streamlines can be determined and the boundaries of the domain are selected to follow the paths shown in Fig. 1 b. The boundary conditions are also imposed using potential flow theory, which allows the flexibility to modify the strain rate and the thermodynamic conditions. The special shape of the computational domain allows one to obtain a high quality mesh with smooth and well controlled stretching. The position of point A (Fig. 1 c) is arbitrary. Point B is on the stream line that crosses point A and only its y-coordinate is arbitrary. Between points B and C, a second order polynomial function is used to get a normal tangent at $y = 0$, and an inflection point in B.
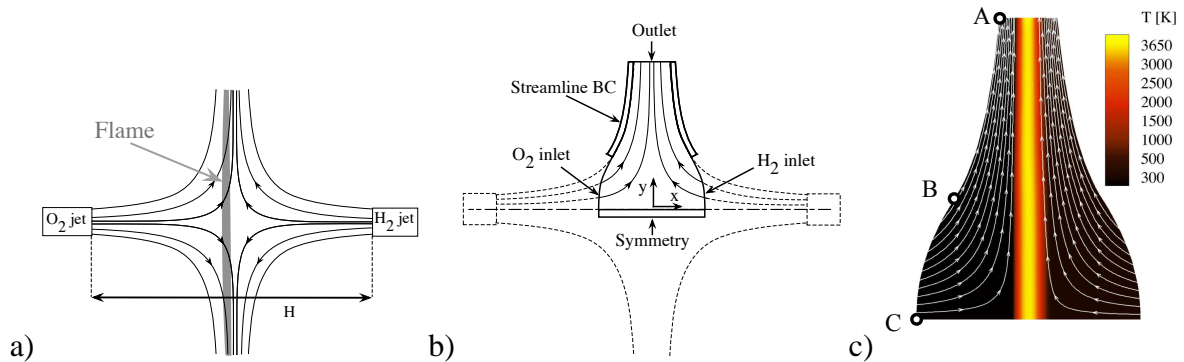

Figure 1. Computational configuration of the two-dimensional counter-flow flame (H is the distance between inlets), a) the theoretical configuration, b) the actual computational domain, and c) flow topology and temperature field of a converged simulation.

This study has been subdivided into five different cases. The first is aimed at validating the present approach and the solver against the Direct Numerical Simulations (DNS) of Ribert *et al.* [21]. These reference computations were computed with a dedicated solver for laminar counter-flow diffusion flame for general fluid conditions (subcritical to supercritical). Cases 2, 3 and 4 focus on the effects of strain, pressure and temperature on the flame structure at rocket-like conditions. Case 5 was selected to investigate real-fluid effects on the reacting flow. For this latter case, the oxygen temperature ($T = 154\,K$) is slightly lower that the critical temperature ($T_{O_2}^c = 155\,K$). By varying the pressure a few bars around the critical pressure ($P_{O_2}^c = 50.4\,bar$),

it is possible to obtain transcritical oxygen ($P = 53\,bar$) or gaseous oxygen ($P = 47\,bar$). Hence, the differences in the flame structure of these two flames only depends on non-idealties of high pressure effects.

3.1. Flame structure : results and discussion

For conciseness, only the main conclusions of Case 1, 2, 3 and 4 are presented in the present paper to allow a more detailed analysis of the real-fluid effects (Case 5).

The strain rate employed for the reference calculations of Ribert *et al.* [21] was $a = 2000\,s^{-1}$, at $50\,bar$. Oxygen and hydrogen were injected at supercritical temperatures ($T_{O_2} = T_{H_2} = 300K$). Good agreement is obtained between the the present approach and the calculations of Ribert. Thus, it was concluded that the present configuration coupled our solver used in a DNS mode can be used to accurately study the flame structure of high pressure hydrogen-oxygen flames. This case also demonstrated that the thermodynamic evaluation scheme used in the present study as well as the cubic equation of state are correctly implemented and give satisfactory results.

The present study is focused on rocket flow where the maximum strain rate is about $a = 10^6\,s^{-1}$. To investigate strain effects on the flame structure, the strain rate was varied from $5 \times 10^4\,s^{-1}$ to $5 \times 10^6\,s^{-1}$. The flame was found to be robust over this range, meaning that the maximum temperature is insensitive to any variation of strain except for $a = 5 \times 10^6\,s^{-1}$. At this strain rate, the maximum temperature decreases slightly due to the fact that the chemical timescale becomes comparable to mixing timescale. In the range of interest $a = 5 \times 10^4\,s^{-1}$; $10^6\,s^{-1}$, the flame is thin and its structure in mixture fraction space is not affected by strain. This implies that the flamelet assumption is valid. It was also shown that in physical space the thickness of the reaction zone (δ_{flame}) follows the asymptotic relation : $\delta_{flame} \propto 1/\sqrt{a}$.

Pressure effects were investigated over the range $53\,bar$ to $90\,bar$. Recall that the critical pressure of oxygen is $P_{O_2}^c = 50.4\,bar$. This range has been chosen to study the effect of pressure oscillations of 30% in a rocket engine operated at $70\,bar$. In mixture fraction space, quantities in the flame front are not impacted by pressure variations. In physical space, the reaction layer, which is a function of the species diffusion term, is sensitive to pressure as $\delta_{flame} \propto 1/\sqrt{P}$. Outside the reaction zone, transport and thermodynamic properties are significantly affected by pressure variations, especially in the region where the dense oxygen heats up. This last observation is a direct consequence of highly nonlinear real-fluid effects.

The impact of inlet temperatures were also studied to measure the flame sensitivity to heat exchange near walls where the oxygen or hydrogen temperatures can increase before entering the flame. Inside the flame zone, temperature and species profiles are almost insensitive to inlet temperature perturbations and significant variations of thermodynamic and transport properties were detected in the cold region on the oxygen side. In this region, the oxygen experiences so-called transcritical-enhancement, where a small variation of temperature can lead to significant modifications of the thermodynamic state.

To investigate the impact of real-fluid effects due to high pressure, inlet temperatures were fixed and thermodynamic conditions were varied by changing the pressure. In the present study, the inlet temperature of oxygen is set at $154\,K$, which is one Kelvin below the critical temperature ($T_{O_2}^c = 155\,K$), and the injection temperature of hydrogen is kept at $295\,K$. One flame is

studied at $47\,bar$, where the oxygen does not experience transcritical effects. A second flame is studied at $53\,bar$ in the transcritical regime and subject to significant nonlinear effects. The locations of these two flames on the $P-T$ diagram of oxygen are shown in Fig. 2.
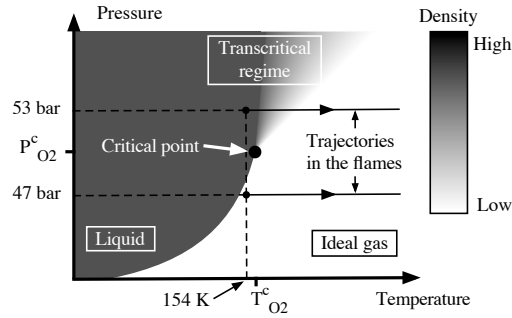

Figure 2. Schematic of the locations of the different flames of Case 5 in the oxygen $P-T$ diagram ($T_{O_2}^c = 155\,K$ and $P_{O_2}^c = 50.4\,bar$).

The first results showing temperature and density in physical and mixture-fraction spaces are given in Fig. 3. In physical space, the temperature profile across the $53\,bar$ flame is slightly narrower than the one at $47\,bar$ due to the effect of pressure on the flame thickness. This effect can be derived asymptotically based on the flamelet approximation. The maximum temperatures of the two flames are the same. The main difference can be observed in the density profiles. For the dense-oxygen flame ($P = 53\,bar$), the injection density of the oxidizer is $587\,kg/m^3$ whereas the light-oxygen flame ($P = 47\,bar$), is fed with a $245\,kg/m^3$ oxygen stream. This difference is a direct consequence of the fact that these two flames are on each side of the saturation curve, as shown in Fig. 2.

Figure 3b shows the temperature distribution across the two flames of interest in mixture-fraction space. For more clarity, the temperature difference indicated in percent has been added to the plot. Non-ideal effects are observed for mixture fraction values around $Z \approx 10^{-3}$, where the difference between the two temperature curves is about 27%. This result first shows that near the critical point, a variation of 11% of the pressure implies a 27% variation of the temperature. Second, for high pressure combustion, the chemistry library must be constructed at the conditions of interest with a solver able to handle non-ideal gas phenomena. For conciseness, species profiles are not shown here. No significant impact of non-ideal effects were observed for the species distributions.

Real fluid effects are further investigated by considering thermodynamic and transport properties. Figure 4 shows the heat capacity at constant pressure (Cp) and the thermal diffusion coefficient across the two flames. Significant differences can be observed for the quantities in the low temperature regions. The heat capacity in the transcritical flame ($p = 53\,bar$) presents a strong peak in the density jump region ($Z \approx 3.10^{-4}$) whereas the Cp profile of the lower pressure flame ($p = 47\,bar$) does not experience such phenomenon. The same observations can be made on the evolution of the thermal diffusion coefficients across the flames, as presented in Fig. 4 b. This thermal barrier is responsible for the difference measured in the temperature profiles in Fig. 3b.

Analysis of these cases reveals that steady laminar counter-flow flames are appropriate to study the flame structure of turbulent oxygen-hydrogen flames at rocket-like conditions. The solver set in DNS mode embeds the required physics required to correctly capture the H_2/O_2
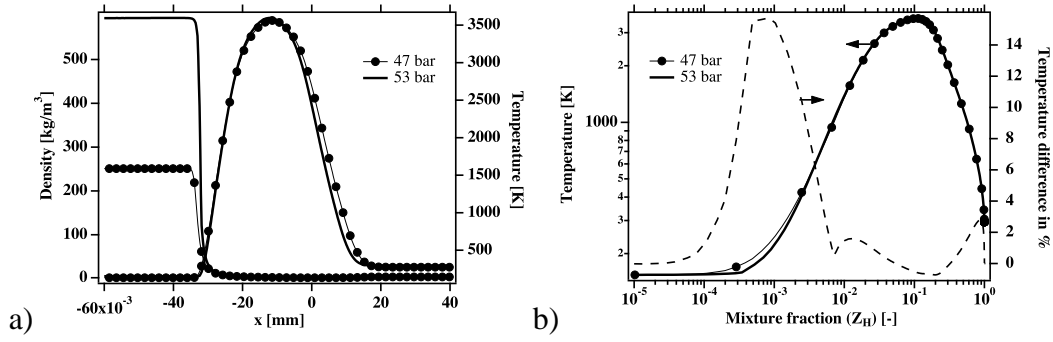
Figure 3. Real fluid effects on the H_2/O_2 counter flow flame. a) Temperature and density distributions in physical space and b) temperature distribution in mixture fraction space. ($T_{O_2} = 154\,K$, $T_{H_2} = 295\,K$ and $a = 10^5\,s^{-1}$).
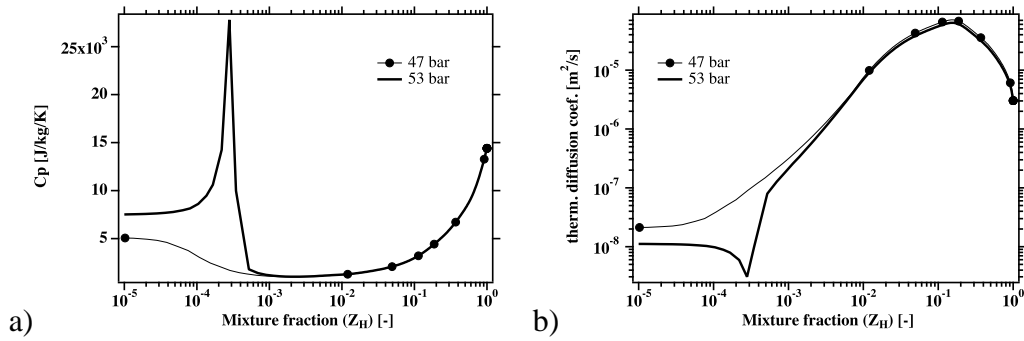

Figure 4. Real fluid effects on thermodynamic and transport properties : a) Heat capacity of the mixture (Cp) and b) thermal diffusion coefficient (D_{th}) in mixture-fraction space ($T_{O_2} = 154\,K$, $T_{H_2} = 295\,K$ and $a = 10^5\,s^{-1}$).

flame structure at high pressure and high strain rate. Effects of strain rate, pressure, temperature and real-fluid phenomena on the flame topology suggest that the flame is robust for the selected conditions, and that the flamelet assumption is valid. A new result shown in the present study is the effect of real-fluid phenomena on the flame structure. For conditions close to the critical point of oxygen, small pressure variations can change the location of the flame in the $P - T$ diagram and the flow can transition from a transcritical regime to a near ideal gas regime. Such modifications of the flow properties have significant impact on the flow, and the flow temperature near the density jump region. For high pressure combustion, real-fluid effects have to be taken into account in the combustion model to correctly capture the destabilization and mixing processes and their interaction with the flame.

Based on these results, it appears that in the flame zone, temperature, and species profiles in Z-space, are almost insensitive to strain, pressure, and inlet temperatures. In the non-reacting areas, pressure and injection temperatures may have a significant impact on transport and thermodynamic properties, and flame temperature. These results are used in the following section to define different combustion model strategies.

4. Model description and performance

The ultimate goal of this study is to develop a combustion model able to reproduce the flame behavior in a rocket engine, where heat loss and pressure waves are present. The direct conse-

quence is that the energy (or enthalpy) transport has to be conserved and the effect of the flame must be represented as a source term $\dot{Q}_E^{model}$. In Section 3 it was shown that the flame temperature is almost insensitive to thermodynamic and flow conditions. Given this, it is possible to define a source term that allows one to recover the correct temperature $\dot{Q}_E^{model} \approx \Gamma \frac{(\rho h_t)^{table} - \rho h_t}{\Delta t}$, where h_t^{table} and ρ^{table} are the total sensitive enthalpy and the density in the flame respectively, Δt is the time step in the computation, and Γ is a test function. The role of the test function is to couple the combustion model with the property evaluation scheme so that in the non-reacting regions the mixture enthalpy is evaluated by the thermodynamic scheme, and in the flame the enthalpy results from the combustion model.

Different model strategies can be employed to account for strain, pressure, temperature and real-fluid effects as follows. The first is a general formulation where several counter-flow flame calculations are required and the input parameters of the table are Z, P and the enthalpy of the mixture. The outputs are the mass and the mixture composition, the transport properties, and the thermodynamic parameters containing the enthalpy of the mixture. The second is the method adopted in the present solver, which embeds the property evaluation scheme in the solver itself (see Section 2.1). To obtain the correct transport and thermodynamic parameters, only the mixture composition is extracted from the tabulation. Pressure and temperature are obtained from transport equations, and the chemistry table is simplified to a one-dimensional manifold $Z \rightarrow (Y_i^{table}, T^{table})$, which can be easily constructed with a single opposed-jet flame calculation. T^{table} is used to evaluate the source term $\dot{Q}_E^{model}$.

4.1. Tabulation strategy

When complex chemistry is used, especially with hydrogen-oxygen combustion, differential diffusion effects are significant and the classical assumption of unity Lewis numbers is inconsistent. One of the main issues is the definition of the mixture fraction Z which is a passive scalar. To circumvent this problem, Bilger defined a mixture fraction based on local element balancing [1]. Another method adopted by Pitsch and Peters is to directly define the passive variable by a conservation equation [18]. The latter has been used in the present study.

In the detailed opposed jet calculations, nine species of the chemical mechanism are transported (H_2, O_2, OH, H_2O, H, O, HO_2, H_2O_2, N_2) and an additional transport equation is added for a passive scalar Z. Decoupling between species and Z ensures correct mapping of the flame structure in Z−space. The Schmidt number of Z (Sc_Z) can be arbitrary. In the present work a unity Lewis number for the mixture fraction is assumed $Le_Z = 1 \Rightarrow Sc_Z = Pr$, as recommended in [18].

4.2. Performance of the model

The model was compared to detailed calculations to assess its performance and sensitivity to strain, pressure and inlet temperatures. Figure 5 presents a comparison in terms of density, temperature and species. The first observation is that the model facilitates recovery of the temperature profile in mixture fraction space. Recalled that the temperature is not directly extracted from the look-up table, but instead from the source term based on enthalpy in the energy equation.

A second observation is that the temperature profile in physical space is in good agreement with the detailed computation. The flame obtained with the model is slightly thinner than the reference flame, but the temperature in the density jump region is recovered correctly. This implies that the density gradient is also correct, as well as the magnitude of the oxygen density in the cold region. The model must preserve the density values in the non-reacting zones of

the flow and in the density gradient close to the flame to accurately capture mixing processes and liquid-oxygen jet interactions with the flow dynamics [5]. Similarly, Figure 5c shows the profiles of the main species extracted from the table. Good agreement is observed between the model and the reference calculation, with minor differences on the hydrogen side.

Figure 6 presents the sensitivity of the model to strain rate, pressure and inlet temperature variations. The previous investigation showed that the strain rate modifies the thickness of the reaction zone due to dynamic effects. Figure 6a confirms that the model reproduces the same trend, giving the correct thickness of the flame region. The sensitivity of the model to pressure variations is also correctly recovered as shown in Fig. 6b. The impact of pressure on the flame thickness is captured with a satisfactory accuracy. These first two results highlight the fact that the model is able to predict heat release fluctuations due to pressure and strain rate variations. This aspect is a requirement to study flame stability in high pressure combustors.

Figure 6c shows the sensitivity of the model to inlet temperature changes. For both oxygen inlet temperatures shown in the figure and the temperature across the flame front is correctly captured by the model. For $T_{O_2} = 300\,K$, the injection temperature is supercritical and thermodynamic and transport coefficients are significantly different from transcritical conditions ($T_{O_2} = 120\,K$). Results in Fig. 6c demonstrate that the model can capture these changes and can be used to investigate the effect of heat exchanges on flame stability.
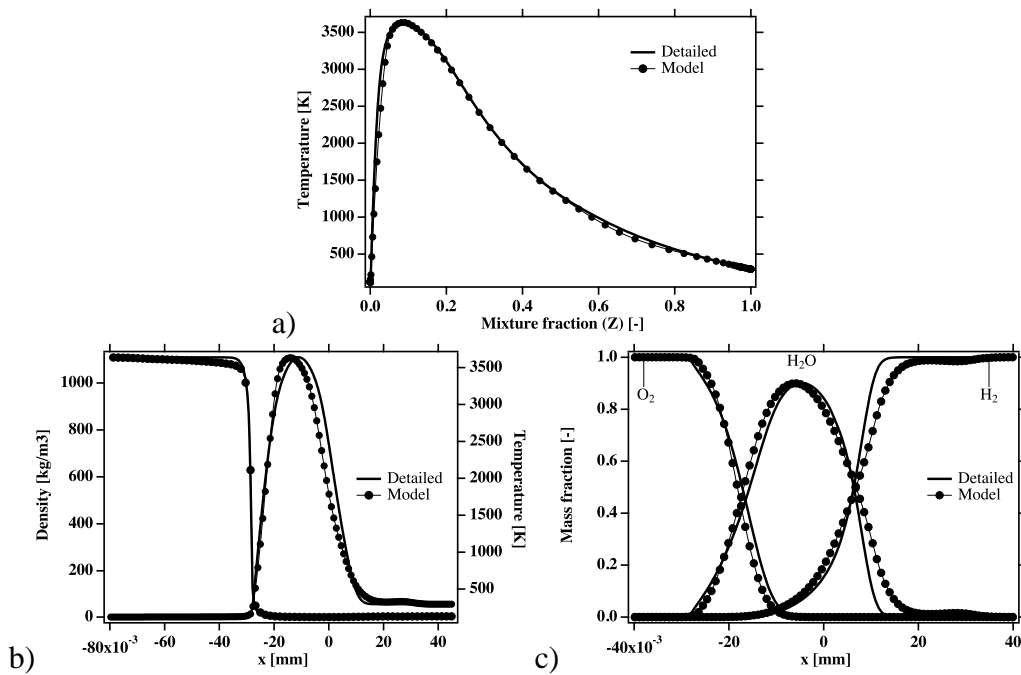

Figure 5. Comparison between the tabulated-chemistry model and the detailed computation. a) Temperature profile in Z-space, b) Temperature and density distributions in physical space and c) mass fraction profiles of major species in physical space ($T_{O_2} = 120K$, $T_{H_2} = 295K$, $P = 70bar$ and $a = 10^5 s^{-1}$).

5. Conclusion

The main objective of the present work was to perform the detailed analysis required for development of a robust model for high-pressure supercritical combustion in high-Reynolds
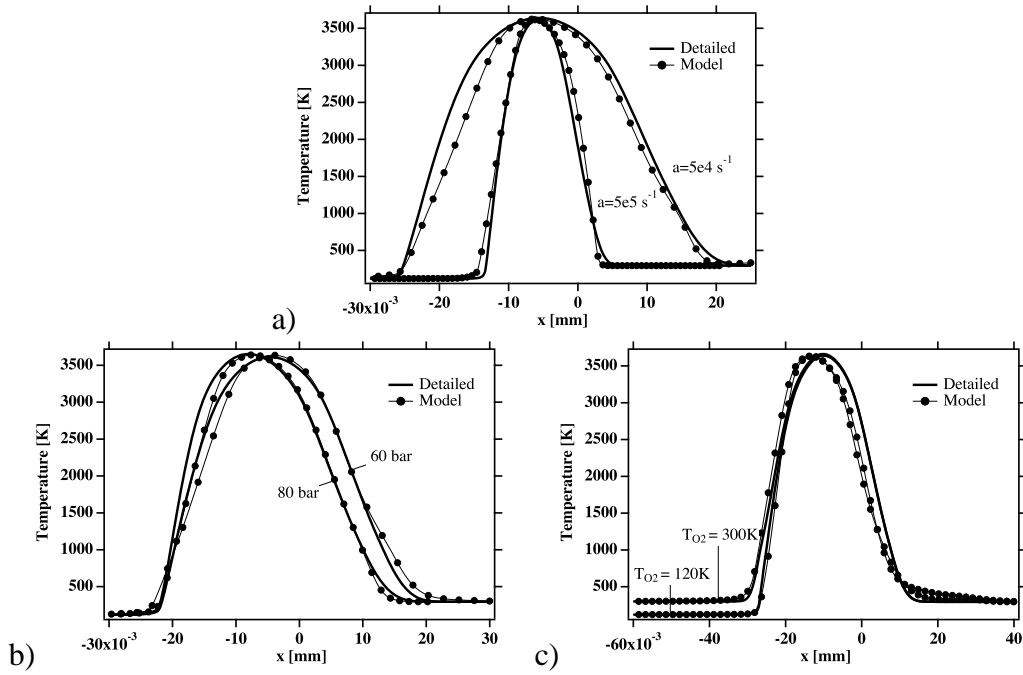
Figure 6. Comparison between the model and the detailed computations : a) Sensitivity of the model to strain rate ($T_{O_2} = 120\,K$, $T_{H_2} = 295\,K$ and $P = 70\,bar$), b) sensitivity of the model to pressure ($T_{O_2} = 120\,K$, $T_{H_2} = 295\,K$ and $a = 10^5\,s^{-1}$) and c) sensitivity of the model to inlet temperature ($T_{H_2} = 295\,K$, $P = 70\,bar$ and $a = 10^5\,s^{-1}$).

number flows. The goal is to treat flame stability in liquid rocket engines with liquid-oxygen and gaseous hydrogen propellants at supercritical pressures. Flame stability in high-pressure devices is affected by both pressure and local strain variations. Thus, to define the most relevant combustion model, the first step was to study the flame structure and its sensitivity to pressure, strain rate and heat losses. The configuration used to perform the analysis was an opposed-jet set-up. Analysis of the trends revealed that the flame is very robust over a large range of strain rates, which implies that the flamelet assumption is valid at least for quasi-steady flow conditions. In addition, it was shown that in the reaction zone, quantities such as temperature, species mass fractions, transport, and thermodynamic quantities are almost insensitive to strain, pressure and inlet temperature variations for the ranges studied. However, pressure and inlet temperatures have a significant impact on properties in non-reacting regions, and especially in the vicinity of the inherently steep density gradients. In the region close to the critical point where thermodynamic nonidealities are predominant, small perturbations in thermodynamic conditions have a strong effect on the overall thermophysical state (i.e., density, temperature, thermodynamics, transport and the coupled interactions with the flow). As a consequence, the model must take these effects into account either directly in the tabulation procedure, or by direct inclusion of the sophisticated property evaluation schemes in the model framework.

Based on these conclusions, a flamelet-like approach has been defined that takes into account both compressibility effects and heat losses. A transport equation for energy is used that includes the heat release source term. The transported quantities are the mixture fraction (Z), density (ρ), total non-chemical energy (E), and the momentum ($\rho\mathbf{u}$). The model strategy then relies on three elements ; 1) a one-dimensional look-up table giving the species and temperature distributions in the flame with respect to the mixture fraction ($Z \rightarrow T^{table}$, Y_i^{table}), 2) a source term that modifies the enthalpy of the flow only in the reaction region to recover the

flame temperature T^{table}, and 3) use of a detailed property evaluation scheme that handles real-fluid thermodynamics and transport for arbitrary mixtures. These elements are coupled to the combustion model and used to determine the thermodynamic and transport properties of the mixture outside of the reaction zone. The model accuracy was tested by implementing it in the LES solver and applying the exact same formalisims in the laminar opposed-jet configuration. Satisfactory agreements were obtained in comparison with the detailed computations. A novel and important result is that the model preserves the density values in the dense oxygen region as well as the density gradient close to the flame. This aspect is of significant importance for the simulation of combustion in practical devices where dense-fluid jet destabilization and mixing are strongly affected by density magnitude and density gradient. Model sensitivity to strain rate, pressure and temperature was also tested and good agreement was obtained in comparison with detailed computations. The next step of this work is to define an appropriate turbulence closure and perform LES computations of practical devices. Several closures will be studied such as presumed-pdf approaches. Different ways to obtained the variance of the mixture fraction will be investigated, from a direct analytical method to a full transport equation approach.

References

[1] BILGER, R. The structure of turbulent nonpremixed flames. *Symposium (International) on Combustion 22*, 1 (1989), 475 – 488.

[2] BOILEAU, M., STAFFELBACH, G., CUENOT, B., POINSOT, T., AND BÉRAT, C. LES of an ignition sequence in a gas turbine engine. *Combustion and Flame 154* (2008), 291–321.

[3] CANDEL, S., JUNIPER, M., SINGLA, G., SCOUFLAIRE, P., AND ROLON, C. Structure and dynamics of cryogenic flames at supercritical pressure. *Combustion Science and Technology 178*, 1 (2006), 161–192.

[4] ELY, J., AND HANLEY, H. J. M. Prediction of transport properties. 2. Thermal conductivity of pure fluids and mixtures. *Industrial & Engineering Chemistry Fundamentals 22*, 1 (1983), 90–97.

[5] HANNOUN, I., FERNANDO, H., AND LIST, E. Turbulence structure near a sharp density interface. *Journal of Fluid Mechanics 189* (1988), 189–209.

[6] HIRSCHFELDER, J., CURTISS, F., AND BIRD, R. *Molecular theory of gases and liquids.* John Wiley & Sons, New York, 1964.

[7] JUNIPER, M., AND CANDEL, S. Edge diffusion flame stabilization behind a step over a liquid reactant. *Journal of Propulsion and Power 19*, 3 (2003), 332–341.

[8] JUNIPER, M., DARABIHA, N., AND CANDEL, S. The extinction limits of a hydrogen counterflow diffusion flame above liquid oxygen. *Combustion and Flame 135*, 1-2 (2003), 87–96.

[9] LINSTROM, P., AND MALLARD, W. *NIST Chemistry WebBook, NIST Standard Reference database*, vol. 69. National Institute of Standards and Technology (NIST), Gaithersburg MD, 20899, 2005.

[10] MAYER, W., AND TAMURA, H. Propellant injection in a liquid oxygen/gaseous hydrogen rocket engine. *Journal of Propulsion and Power 12*, 6 (1996), 1137–1147.

[11] MOIN, P., AND APTE, S. V. Large-eddy simulation of realistic gas turbine combustors. *American Institute of Aeronautics and Astronautics Journal 44*, 4 (2006), 698–708.

[12] ÓCONAIRE, M., CURRAN, H., SIMMIE, J., PITZ, W., AND WESTBROOK, C. A comprehensive modeling study of hydrogen oxidation. *International Journal of Chemical Kinetics 36*, 11 (2004), 603–622.

[13] OEFELEIN, J. Large eddy simulation of turbulent combustion processes in propulsion and power systems. *Progress in Aerospace Sciences 42*, 1 (2006), 2–37.

[14] OEFELEIN, J. C. Les of supercritical lox-h2 injection and combustion in a shear coaxial uni-element rocket. *41st Aerospace Sciences Meeting and Exhibit*, AIAA-2003-0479 (Jan. 2003).

[15] OEFELEIN, J. C. Thermophysical characteristics of shear-coaxial lox–h2 flames at supercritical pressure. *Proc. Combust. Inst. 30*, 2 (2005), 2929–2937.

[16] OEFELEIN, J. C. Mixing and combustion of cryogenic oxygen-hydrogen shear-coaxial jet flames at supercritical pressure. *Combustion Science and Technology 178*, 1-3 (2006), 229–252.

[17] OEFELEIN, J. C. *General package for evaluation of multicomponent real-gas and liquid mixture states at all pressures*. Sandia National Laboratories, Livermore, CA, 2009.

[18] PITSCH, H., AND PETERS, N. A consistent flamelet formulation for non-premixed combustion considering differential diffusion effects. *Combust. Flame 114* (1998), 26–40.

[19] POINSOT, T., AND LELE, S. Boundary conditions for direct simulations of compressible viscous flows. *Journal of Computational Physics 101*, 1 (1992), 104–129.

[20] REID, R. C., PRAUSNITZ, J. M., AND POLLING, B. E. *The properties of liquids and gases*, vol. fourth ed. McGraw Hill, New York, 1987.

[21] RIBERT, G., ZONG, N., YANG, V., PONS, L., DARABIHA, N., AND CANDEL, S. Counterflow diffusion flames of general fluids: Oxygen/hydrogen mixtures. *Combustion and Flame* (2008), 319–330.

[22] SINGLA, G., SCOUFLAIRE, P., ROLON, C., AND CANDEL, S. Planar laser-induced fluorescence of OH in high-pressure cryogenic LOx/GH2 jet flames. *Combustion and Flame 144*, 1-2 (2006), 151–169.

[23] TAKAHASHI, S. Preparation of a generalized chart for the diffusion coefficients of gases at high pressures. *journal of Chemical Engineering of Japan 7*, 6 (1974), 417–420.